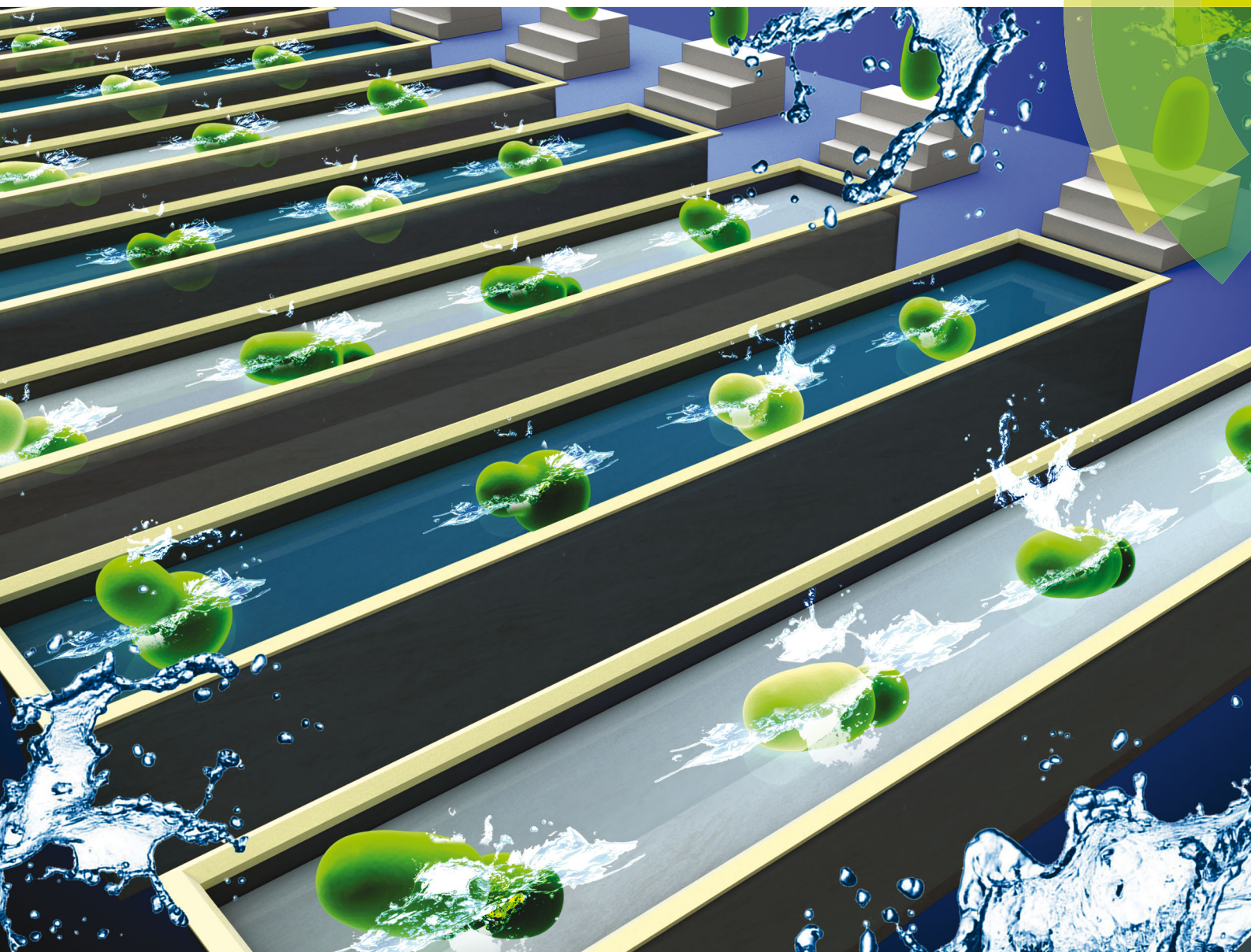


Integrative Biology

Interdisciplinary approaches for molecular and cellular life sciences

www.rsc.org/ibiology



ISSN 1757-9694



ROYAL SOCIETY
OF CHEMISTRY

PAPER

Chunxiong Luo *et al.*

Protein expression patterns of the yeast mating response

**Indexed in
Medline!**



Cite this: *Integr. Biol.*, 2016, 8, 712

Protein expression patterns of the yeast mating response†

Haiyu Yuan,^a Rongfei Zhang,^b Bin Shao,^{ab} Xuan Wang,^{ab} Qi Ouyang,^{abc} Nan Hao^d and Chunxiong Luo^{*ab}

Microfluidics, in combination with time-lapse microscopy, is a transformative technology that significantly enhances our ability to monitor and probe biological processes in living cells. However, high-throughput microfluidic devices mostly require sophisticated preparatory and setup work and are thus hard to adopt by non-experts. In this work, we designed an easy-to-use microfluidic chip, which enables tracking of 48 GFP-tagged yeast strains, with each strain under two different stimulus conditions, in a single experiment. We used this technology to investigate the dynamic pattern of protein expression during the yeast mating differentiation response. High doses of pheromone induce cell cycle arrest and the shmoo morphology, whereas low doses of pheromone lead to elongation and chemotrophic growth. By systematically analyzing the protein dynamics of 156 pheromone-regulated genes, we identified groups of genes that are preferentially induced in response to low-dose pheromone (elongation during growth) or high-dose pheromone (shmoo formation and cell cycle arrest). The protein dynamics of these genes may provide insights into the mechanisms underlying the differentiation switch induced by different doses of pheromone.

Received 26th January 2016,
Accepted 27th April 2016

DOI: 10.1039/c6ib00014b

www.rsc.org/ibiology

Insight, innovation, integration

An easily operated high-throughput microfluidic chip was designed to realize the confinements of 48 different GFP-tagged yeast strains under two different conditions. Using this chip, we systematically studied the protein expression patterns of the mating pathway under high-dose (shmoo state) and low-dose (elongation state) alpha-factor treated conditions. By cluster analysis and comparing the dynamic response of the 156 mating related protein expression level between shmoo states and elongation states, proteins which have similar and obviously different performance in the two different states were discussed, which may contribute to the understanding of mating pathway networks.

1. Introduction

Cells respond to extracellular signals through intercellular signaling pathways. To help the cell adapt to the new environments, the reactions of the proteins involved in the signaling pathway often have dynamic features. Systematic studies of dynamic protein expression patterns after external stimulation may confine the possible signaling pathway networks and reveal the underlying mechanisms of the signaling networks.

The budding yeast mating pathway is a typical mitogen-activated protein kinase (MAPK) system that plays an important role in many other cellular processes.¹ The studies of the yeast mating pathway have revealed important information about eukaryotic signaling networks.^{2–5} In addition, yeast would exhibit different phenotypes depending on the extracellular pheromone concentration.^{6,7} This phenomenon makes the yeast mating pathway a prototypical cell fate decision process.

The pheromone-induced behaviour in yeast cells involves important biological processes, such as cell mating, cell polarization and cell fusion. The mating pathway in yeast cells has been studied for decades, and the primary process before transcription is almost completely understood (Fig. 1). An extracellular pheromone can be recognized by a receptor in the cell membrane, and then the signal is transmitted through the MAPK cascade involving the proteins STE5, STE11, STE7, FUS3 and KSS1. Eventually, the transcription factor STE12 would be activated, and bind to the pheromone response element (PRE), and then regulate the

^a The State Key Laboratory for Artificial Microstructures and Mesoscopic Physics, School of Physics, Peking University, China. E-mail: pkluocx@pku.edu.cn; Tel: +86-10-62754743

^b Center for Quantitative Biology, Academy for Advanced Interdisciplinary Studies, Peking University, China

^c Peking-Tsinghua Center for Life Sciences, Peking University, Beijing, 100871, China

^d Section of Molecular Biology, Division of Biological Sciences, University of California San Diego, La Jolla, CA 92093, USA

† Electronic supplementary information (ESI) available. See DOI: 10.1039/c6ib00014b

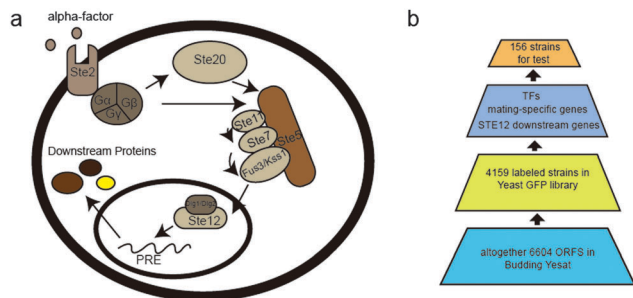


Fig. 1 (a) Mating signaling in a-type budding yeast. The STE2 receptor in the membrane binds the alpha-factor, causing the release of the $G\beta\gamma$ heterodimer from the G-protein heterotrimer. Then, the $G\beta\gamma$ protein binds to STE20 and the STE5 scaffold protein. The STE5 protein activates the downstream kinases STE11, STE7 and FUS3 or KSS1, which promote the release of DIG1 or DIG2 from STE12. STE12 binds to the pheromone response element (PRE) and activates downstream proteins, including transcription factors and functional proteins. (b) The process of selecting 156 genes for testing. Altogether, there are 6604 ORFs in budding yeast, and we have 4159 strains in our library, in which every strain represents one type of GFP-fused protein. We chose 72 STE12 downstream genes from the *Saccharomyces* Genome Database and a previous paper.¹⁸ We chose 52 mating-specific genes from a mRNA expression database⁹ and the *Saccharomyces* Genome Database. We also chose 41 important transcription factors (TFs) from the *Saccharomyces* Genome Database. However, 9 genes overlapped between these three sources.

transcription of downstream proteins. In this process, the transcription factor STE12 plays a central role in the yeast mating pathway.³

When exposed to different pheromone concentrations, yeasts would show different morphological changes. Two normal phenotypes are shmoo growth and elongation growth, which can be clearly distinguished phenomenologically. When yeast cells are exposed to a high dose of pheromone, the cells undergo cell arrest and form a pear-like shape termed 'shmoo'.^{6,8} In contrast, under low-dose conditions, cells undergo temporary cell arrest, elongate from one position and form elongated cylindrical shapes termed 'elongation'.⁸ We speculated that cells employ different proteins or trigger different protein expression patterns, leading to the two different phenotypes, although these proteins are mainly regulated by the same transcription factor, STE12. These different protein expression patterns should be important for revealing the mechanisms underlying the mating pathway.

Several technologies have been used to study the yeast mating pathway at the mRNA or protein expression level, such as the DNA microarray method,⁹ mass spectroscopy technology,¹⁰ western blot and genetic manipulation.¹¹ However, these methods are limited by low time resolution and the lack of measurements in living-cells, and the DNA microarray method cannot reveal the protein expression level because of the fact that the mRNA level has little correlation with protein expression.^{12,13} The mass spectroscopy and western blot methods cannot measure the expression of large numbers of proteins conveniently. The microfluidic chip method has the advantage of high time resolution and the allowance of high-throughput experiments in one chip.^{14,15} Recently, one microfluidic chip has been used to measure the yeast response to changing alpha-factor

environments for different genetic perturbations.¹⁶ However, the fabrication and operation of this chip are very complex. Moreover, only a few gene-knockout strains can be loaded and used to study gene functions at the same time. Here, we provided a novel microfluidic device to overcome these disadvantages and perform a high-throughput protein dynamic expression study. Our method can record the dynamic of the protein expression of 48 different GFP-tagged yeast strains under two conditions at the same time. Using batch image processing software, we obtained and compared the relative dynamic expression patterns of 156 mating pathway proteins for the shmoo and elongation phenotypes and finally identified certain proteins that exhibited the greatest difference in dynamic expression patterns between the two phenotypes.

2. Materials and methods

Strains and cell culture

The a-type budding yeast cells we used were from a collection of *S. cerevisiae*-tagged open reading frames (ORFs) generated by Dr. Erin O'Shea and Dr. Jonathan Weissman at UCSF.¹⁷ The strains in the collection are GFP-tagged which means that green fluorescence intensity can reflect the target protein concentration. Thus, this is an excellent tool for analyzing the response of one specific protein to external stimuli. According to previous papers, we chose 156 potentially important proteins that had an obvious fold change in DNA microarray experiments or are downstream proteins of the gene STE12 as determined by mass spectrometry (MS) technology, or are important transcription factors (Fig. 1(b)).^{9,18} The names of labelled proteins are listed in the ESI†. The corresponding strains we used contain the *Schizosaccharomyces pombe* His5⁺ gene, so we used SD medium (His⁻) to culture yeast cells for approximately 8 hours before experiments. When the yeast cells are in the exponential phase, we can load the cells into our microfluidic chip and begin the experiment.

Microfluidic chip design and operation

We designed and fabricated a high-throughput microfluidic chip for our experiment (Fig. 2(b)). One microfluidic chip contains 96 parallel channels, and we can load strains into different channels. The loaded strains can be fixed well in the observation chamber in each channel (approximately 4 μm high, 200 μm wide; yellow area in Fig. 2(c)) because the size of the yeast is similar to the height of the observation chamber. The strains in the upper 48 channels are in the same culture environment, and the strains in the lower 48 channels are in the other culture environment. At the end of the observation chamber, there are necks (approximately 8 μm wide, 2 μm high; green parts in Fig. 2(c)). The loaded cells cannot pass the necks, but the cell culture medium can travel through the necks towards the observation chambers.

After the microfluidic chip was degassed in a vacuum for 15 min, the yeast cells were directly loaded from loading holes into the observation chamber using a 10 μl pipette. The culture medium can be injected from four inlets to all the channels

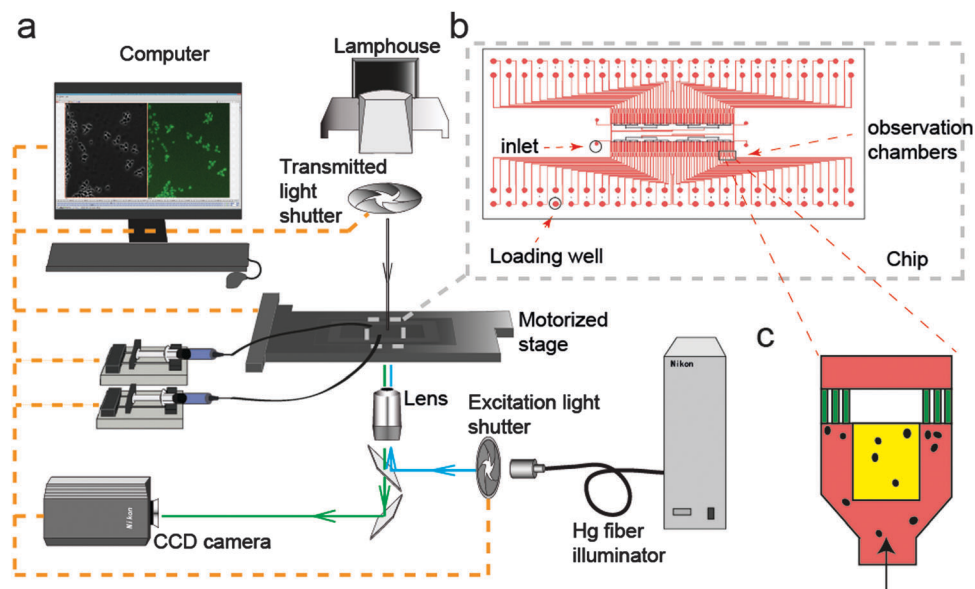


Fig. 2 Schematic of our system containing (a) a computer system with specific software, a Nikon Ti-E microscope, syringe pumps and (b) a microfluidic chip. (c) Schematic diagram of the observation chambers and necks. The green parts are 2 μm -high necks. The yellow area is a 4 μm -high chamber. The red part is a 20 μm -high channel.

through pumps with a constant flow rate of 400 $\mu\text{l h}^{-1}$. After all the strains were loaded into the observation chambers, yeast cells were cultured in SD medium in the microfluidic chip for approximately 60 minutes before the medium containing the alpha-factor was injected into the chambers (more details of the device design, fabrication and operation can be found in the ESI† and Fig. S1).

System setup and automated image acquisition

We set up an automated image acquisition system using a Nikon Ti-E microscope, a computer system and syringe pumps (Fig. 2(a)). The system can automatically acquire phase difference and fluorescence images in 96 selected positions through NIS-Elements advanced research software. We obtained a series of images for all 96 positions, and the time interval between two images was 5 minutes. The entire process of image acquisition would take 10 hours. The temperature was maintained at 30 $^{\circ}\text{C}$ throughout the entire experiment using a temperature control system.

Image processing and data processing

Using our microfluidic chip and image acquisition system, we could obtain sequential phase difference pictures and fluorescence pictures containing more or fewer yeast cells (Fig. 3(a)). In the phase difference pictures, the intracellular region appears black, while the cell margin was bright white and the extracellular region was also black. This feature helps to distinguish the cellular region in the phase difference picture. We used the Dynamic Directional Gradient Vector Flow (DDGVF) algorithm,¹⁹ which has been widely used in cell segmentation for precise identification of cell margin; then we could obtain mask pictures that cover the yeast cells (Fig. 3(d)). Using mask pictures, phase difference pictures and fluorescence pictures (Fig. 3(b)), we could also track yeast cells and

read out the cellular GFP concentration using a Matlab program provided by the lab Hao Nan Lab at UCSD; thus, the average GFP concentration data could be obtained eventually (Fig. 3(c)). Although we could obtain single-cell protein expression data, we did not focus our attention on this information; instead, we studied the average protein expression of approximately 20–50 cells.

3. Results and discussion

3.1 Experimental results

We tested the expression profiles of 156 mating pathway related proteins under high-dose and low-dose alpha-factor conditions, which induce shmoo formation and elongation formation, respectively. The concentration of the alpha-factor pheromone was 10 $\mu\text{g ml}^{-1}$ or 1 $\mu\text{g ml}^{-1}$, respectively, under the high-dose or low-dose conditions. Our test and previous papers indicate that the high-dose concentration of 10 $\mu\text{g ml}^{-1}$ is a saturating concentration for yeast shmoo formation, and the low-dose condition is suitable for elongation state formation.²⁰ Fig. 4(a) and (b) show the expression patterns of the 156 proteins. Our results demonstrate that for most of the proteins, the expression is up-regulated in both the shmoo and elongation states. For the shmoo state, 117 proteins have a fold greater than 1.5, and 61 proteins have a fold change greater than 2. For the elongation state, 116 proteins have a fold change greater than 1.5 and 53 proteins have a fold change greater than 2. The expression was down-regulated or unchanged for only a few of the tested proteins. However, for some proteins, the expression profile clearly differs between the shmoo and elongation states. We can depict this difference quantitatively in the response time, response amplitude and dynamic patterns. We also compared our results with previous data from the DNA microarray method.⁹

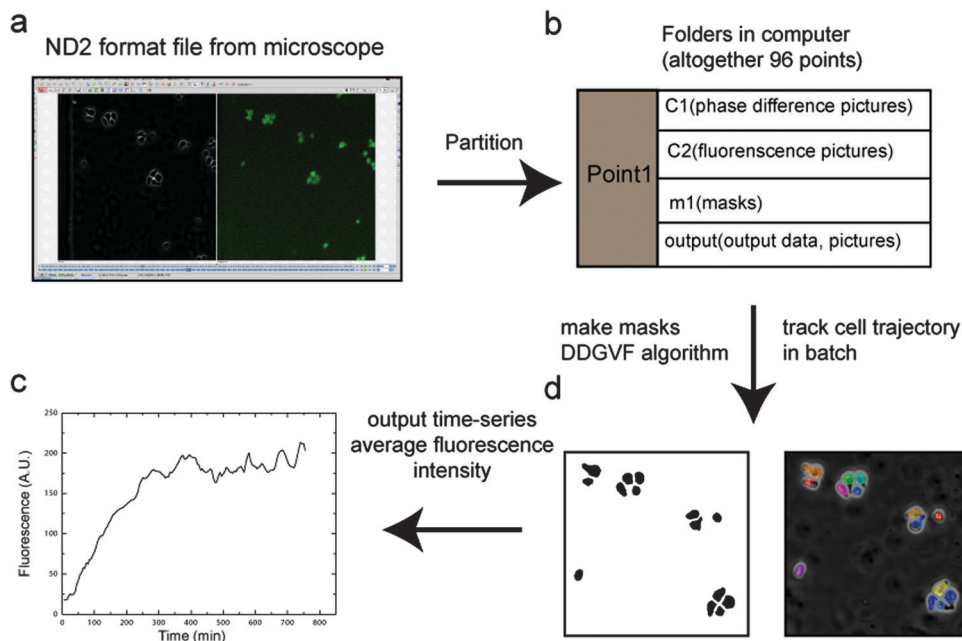


Fig. 3 Schematic diagram of image processing for microscope-captured pictures. (a) The ND2 format file we obtained from the microscope software. (b) The ND2 format file can be divided to 23 232 ($121 \times 96 \times 2$) pictures using NIS-Elements AR software. We created 96 folders in the computer, and each folder contained four subfolders, C1, C2, m1 and the output. In total, 121 phase difference pictures were placed in folder C1, and 121 fluorescence pictures were placed in folder C2. Folder m1 was produced to hold the mask pictures from the next step. The output folder was produced to hold the output data and pictures from the next step. This entire process is automated using one Python script. (c) Using a Matlab program provided by the lab of Hao Nan at UCSD, we could automatically perform mask production (based on the DDGVF algorithm), cell tracking, the picture output (merging of phase difference pictures and a colored mask) and the data output. The mask pictures, output pictures and output data were placed in two different folders. (d) Based on the output data from the last step, we could obtain the time-series area-average fluorescence value of a single cell. Eventually, we could calculate the time-series average fluorescence values of all the cells in one observation chamber and plot the protein expression curve.

Because mRNA expression data have poor time resolution and a short observation time (120 minutes) and because only data on high-dose alpha-factor treatment are available, we compared the fold change of protein expression with that of mRNA expression during the 120 minute period after high-dose alpha-factor treatment. In our experiment, 61 proteins have a fold change greater than 1.5. In the DNA microarray experiment, only 14 of these 61 genes had a fold change greater than 1.5, and only 20 had a fold change greater than 1. We conclude that the mRNA expression is not very consistent with the protein expression. Some previous papers have already reported the weak correlation between protein and mRNA expression.^{12,13} Our comparison supported this opinion. At the protein level, the protein KSS1, which has an important role in the mating pathway, has a fold change greater than 2 in both the shmoo and elongation states, a finding that is similar to the results of previous research.²⁰ Additionally, the protein FAR1, which is involved in pheromone response and is necessary for cell cycle arrest, also has a fold change greater than 2 in the shmoo state, which is also similar to the results of previous research.²¹

3.2 Quantitative study of the protein expression level differences between different conditions

Because most of the proteins were up-regulated, we selected the maximum value of the fluorescence intensity and the response

amplitude as useful measurements of protein expression. We constructed one index R to measure the difference in expression between the high- and low-dose conditions. The formula for R is

$$R = \log_2 \left(\frac{m1}{m2} \right)$$

In this equation, $m1$ is the maximum value of the mean fluorescence intensity for the shmoo state, while $m2$ is the maximum value of the mean fluorescence intensity for the elongation state.

We calculated the R values for every protein we tested and ranked these proteins based on the R values (Table 1). A greater R value means a protein has a stronger response in the shmoo state than the elongation state. In contrast, a smaller R value means a protein has a stronger response in the elongation state than the shmoo state. The proteins in the upper region of Fig. 4(a) and (b) have large R values and higher expression in the shmoo state (Fig. 4(a)). The proteins in the lower region of Fig. 4(a) and (b) have small R values and higher expression in the elongation state (Fig. 4(b)). The proteins in the middle region of Fig. 4(a) and (b) have R values close to zero but a shorter time between the treatment and the peak expression in the shmoo state than the elongation state.

From the distribution graph of the R values (Fig. 4(c)), we find that most of the R values are close to zero which means

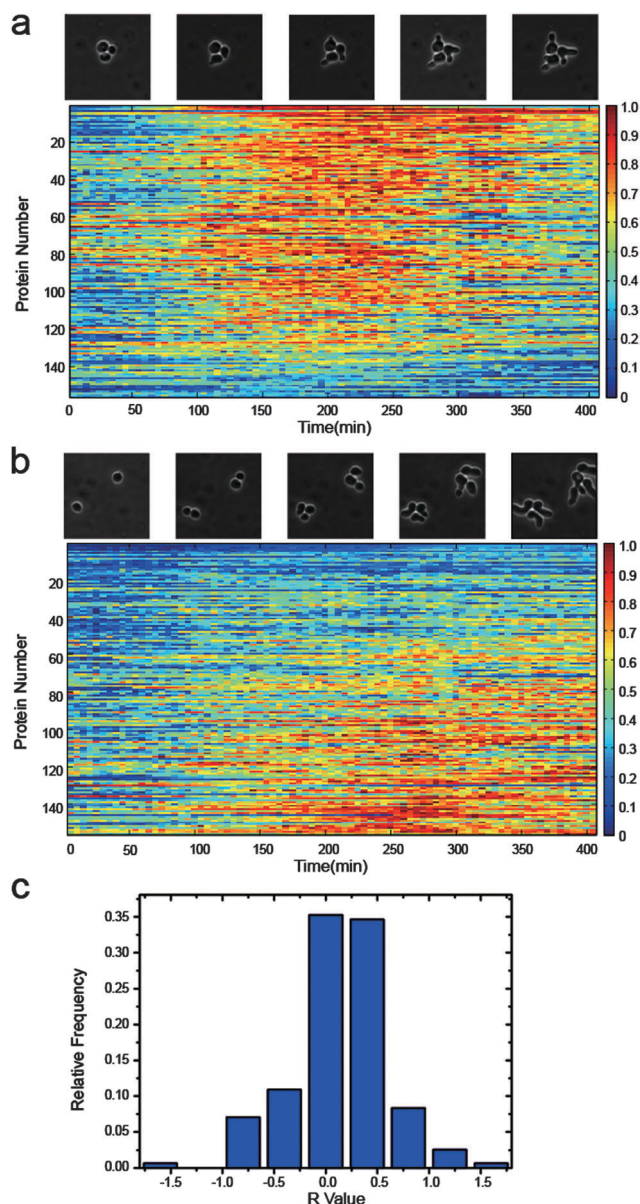


Fig. 4 Diagrams showing the protein expression and the distribution graph of the R value. (a) Dynamic protein expression patterns in the shmoo state containing 400 minutes after the alpha-factor input (sorted by the R value). (b) Dynamic protein expression patterns in the elongation state (sorted by the R value). The protein expression of every protein in (a and b) is normalized using both the largest and smallest fluorescence values for the two phenotypes. For each protein, the largest fluorescence value of the two phenotypes is normalized to 1. The smallest fluorescence value of the two phenotypes is normalized to 0. The other fluorescence values are normalized based on a linear transformation. (c) Distribution graph of the R values of 156 proteins.

that the difference between the two states is not significant for these proteins. There are more proteins that have a positive R value than a negative R value. On average, the protein expression in the shmoo state is higher than in the elongation state. Additionally, the largest R value is approximately 1.7, and the smallest R value is approximately -1.5 . We chose the 15 proteins with the largest R values and the 15 with the smallest R values

Table 1 Table of selected proteins. (a) The fifteen proteins with the largest R values. (b) The fifteen proteins with the smallest R values

(a)		(b)	
Protein name	R value	Protein name	R value
YIL083C	1.76	HIR3	-0.47
MFA1	1.22	DOT6	-0.51
TEC1	1.22	PRP39	-0.55
KSS1	1.21	MIG1	-0.61
UME6	1.10	AGA1	-0.62
CAC2	0.93	STE2	-0.65
ECM18	0.86	RAD51	-0.69
PPH3	0.84	RLM1	-0.70
CSE4	0.83	SSF2	-0.73
ZAP1	0.75	YKL222C	-0.74
YMR204C	0.73	MSI1	-0.87
ASN1	0.73	BEM4	-0.87
CRH1	0.69	HCM1	-0.91
STE11	0.67	SPT10	-0.95
YLL013C	0.67	LEU3	-1.52

because these proteins have the largest relative difference in the dynamic expression patterns between the two different states. Furthermore, these proteins may have different functions in the mating pathway network when the concentrations in the external environment are significantly different. Fig. 5 shows the expression curves of some proteins in the two states. Fig. 5(a) shows the proteins YIL083C, Ume6 and KSS1, all of which have a large R value. Fig. 5(b) shows the proteins Hir3, Leu3 and YKL222C, all of which have a small R value. Fig. 5(c) shows the proteins CDC39, HAL9 and GAL11, all of which have an R value close to 0. Fig. 5(d) and (e) show pictures of the proteins KSS1 and YKL222C, whose R values are 1.21 and -0.74 , respectively. Under high-dose stimulation, yeast cells undergo shmoo formation and the protein KSS1 would be expressed more rapidly and at higher levels (Fig. 5(d)). In contrast, for the low-dose stimulation, yeast cells undergo elongation formation, and the protein YKL222C would be expressed at higher levels.

Based on the calculated R values, the proteins YIL083C, MFA1, TEC1, KSS1, UME6, CAC2, ECM18, PPH3, CSE4, ZAP1, YMR204C, ASN1, CRH1, STE11, YLL013C are the most highly regulated in the shmoo state compared to the elongation state (Table 1). All of the fifteen proteins are up-regulated in the shmoo state, and most of the fifteen proteins are not regulated in the elongation state. The proteins KSS1, MFA1, CAC2, TEC1, PPH3 and ZAP1 are also up-regulated in the elongation state, but the increases in the expression of these proteins are smaller than in the shmoo state. The protein MFA1 is an essential protein excreted by α -type yeast cells to act on α -type yeast cells, and this protein is involved in conjugation with cellular fusion.²² The protein MFA1 has a stronger response in the shmoo state, possibly because yeast cells feel a stronger signal from other types of cells and produce more MFA1 protein to act on other types of cells. The gene STE11 and KSS1 are major proteins that participate in the mating pathway.³ The gene TEC1 can bind to the transcription factor STE12 and form a complex to exert biological effects.²³ The gene PPH3 participates in the regulation of many biological processes, such as glucose-mediated signaling pathways, nitrogen compound metabolic processes and the meiotic recombination checkpoint.^{24–26}

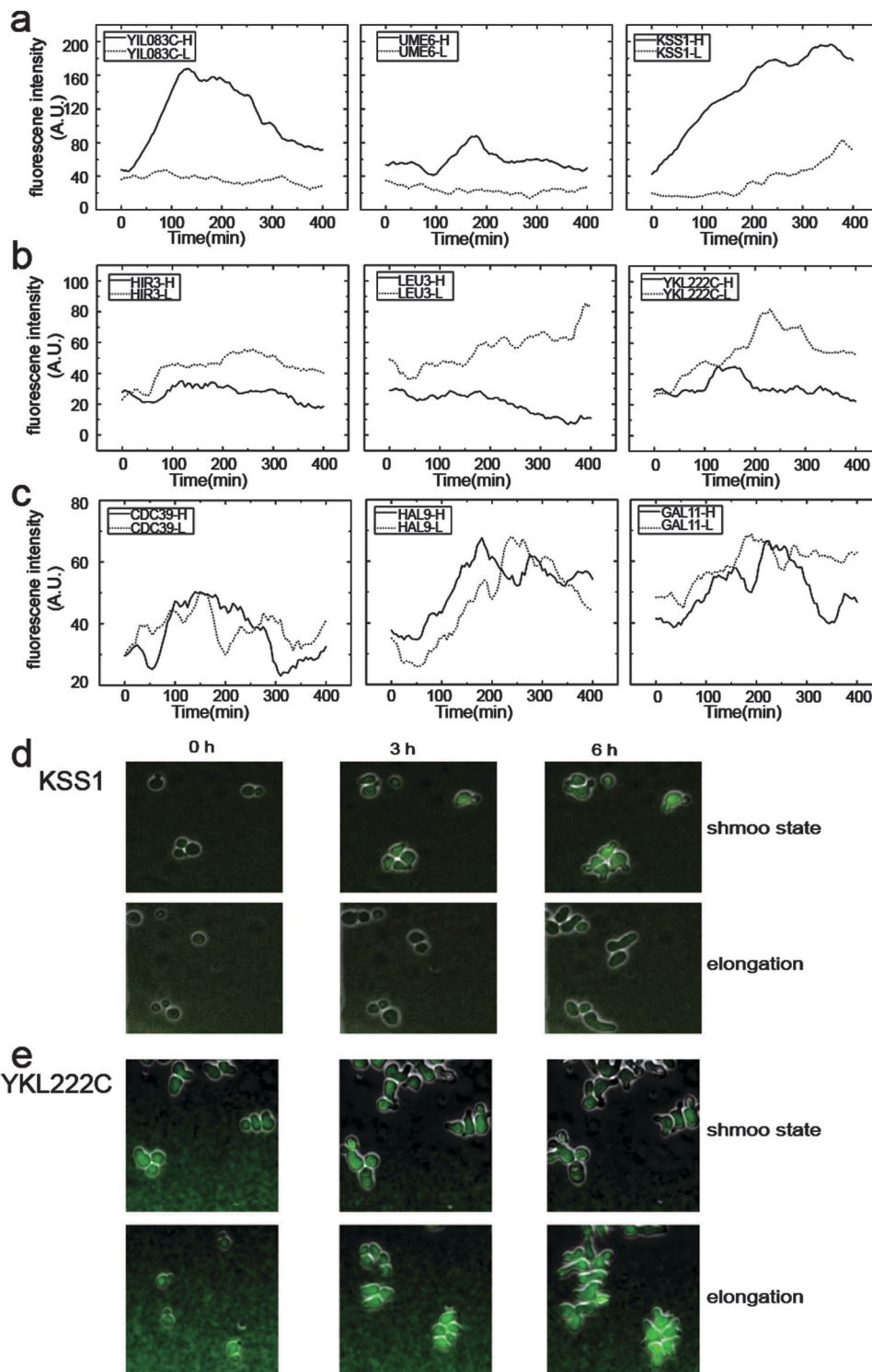


Fig. 5 Expression results of some example proteins. (a) Expression curves of three proteins with large R values for the two phenotypes. The suffix H and solid lines represent the high-dose condition and the shmoo state. The suffix L and dotted lines represent the low-dose condition and the elongation state. We add the alpha-factor to the channels at time 0. (b) Expression curves of three proteins with small R values for the two phenotypes. We add the alpha-factor to channels at time 0. (c) The expression curves of the two phenotypes of three proteins that have an R value close to 0. (d) Phase difference pictures merged with fluorescence pictures of the protein KSS1 in the shmoo and elongation states. (e) Phase difference pictures merged with fluorescence pictures of the protein YKL222C in the shmoo and elongation states.

However, some other genes, such as LEU3, SPT10, HCM1, MIG1, PRP39, DOT6 and HIR3 have a stronger response in BEM4, MSI1, YKL222C, SSF2, RLM1, RAD51, STE2, AGA1, the elongation state than in the shmoo state (Table 1). RLM1 is

a transcription factor that is regulated by the cell wall integrity MAP kinase.²⁷ RLM1 regulates at least 25 downstream genes, most of which are related to cell wall biogenesis.^{27,28} Our experimental data indicate that when cells are exposed to pheromone, the RLM1 protein is up-regulated under both high-dose and low-dose conditions. However, the *R* value of RLM1 is very low, which means that yeast cells express more RLM1 protein under low-dose conditions than high-dose conditions. This finding is consistent with the fact that the cells would experience more cell wall synthesis stress during elongation growth. Oxidative stress can also activate RLM1 transcription in yeast cells.²⁷ This finding shows that RLM1 is up-regulated by different stresses and that the RLM1 protein is an important product of different stress response pathways. Among the other genes, BEM4 is involved in the control of polarized growth and bud emergence and is a negative regulator of the mating pathway.²⁹ The gene DOT6 is related to transcriptional regulation, cell cycle progression and developmental events.^{30,31} The genes SSF2 and AGA1 are related to cellular fusion.^{32,33} However, previous studies suggest that some other genes may not directly play a role in the mating process. For example, HIR3 is a repressor of histone gene transcription,³⁴ MSI1 is a component of chromatin assembly factor1 (CAF-1),³⁵ LEU3 is a factor that controls a group of leucine-specific genes,³⁶ SPT10 is required for some transcriptional regulation in yeast,³⁷ and RAD51 is a DNA repair protein.³⁸ We speculate that these proteins may have unknown functions in pheromone-induced elongation growth.

3.3 Cluster analysis using the dynamic data of 156 proteins

We used cluster analysis method to analyze our protein expression data by the Matlab clustergram function (Fig. 6). Fig. 6(a) shows the protein clusters in the shmoo state. We could recognize that there are several clusters using our data (Fig. 6). We found a lot of proteins that have similar biological functions which would be classified into one cluster. For example, proteins SFP1, BDF2 and RCS1 were all related to DNA replication stress and these proteins were all clustered in the adjacent positions in the up region in Fig. 6(a). We labeled the three largest clusters with yellow (cluster 1), red (cluster 2), green (cluster 3) colors in Fig. 6(a). Cluster 1 represents that the protein expression was activated firstly, and then adapted. Cluster 2 represents that the protein expression was down-regulated after alpha-factor treatment. Cluster 3 represents that the protein expression was also activated but maintained in the activated state for a longer time than cluster 1. We found that some growth-relevant proteins were classified into cluster 2, such as RIM101, AZF1, MIG1. These proteins were down-regulated since cells' growth rate would decrease after alpha-factor treatment. Most of the proteins directly related to the mating pathway were classified into clusters 1 or 3. These proteins were up-regulated but would perform at different response times and duration times in the activation state. Most of the proteins associated with cell wall integrity and synthesis were in cluster 3. Most of the proteins related to stress response were in clusters 1 or 3. Specifically, the proteins related to osmotic stress and oxidative stress were in cluster 1.

Fig. 6(b) shows the protein expression in the elongation state. We found that the time between treatment and the peak

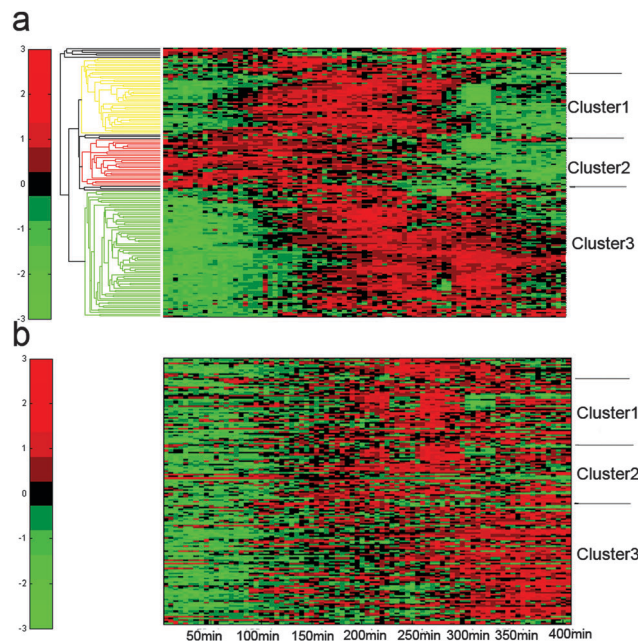


Fig. 6 Cluster analysis by the protein dynamic data of the shmoo state. (a) Protein expression data in the shmoo state. We could recognize three main clusters using dynamic data. We injected the alpha-factor at time $t = 0$. (b) Protein expression data in the elongation state. In (b), we maintained the protein order as to compare with (a).

expression was longer in the elongation state than in the shmoo state in clusters 1 and 3. In cluster 2, most of the proteins were not down-regulated in the elongation state. This shows that the proteins showed different dynamic behaviors between shmoo and elongation states. Using the cluster analysis method, we could find some modules in the mating process and this would deepen our understanding about the protein function and the underlining protein regulation network.

4. Conclusion

Using our designed microfluidic chip and constructed observation system, we successfully measured the expression response process of potential significant proteins in the yeast mating pathway and obtained the protein expression patterns for two phenotypes. Based on our calculated protein *R* values, we selected the proteins that have the greatest different in performance between different cell states from all the proteins tested.

In our experiment, most of the proteins were up-regulated, as indicated by the average GFP concentration. However, in both the shmoo and elongation states, we observed a growth rate change that might increase the average GFP concentration. This situation is not a major problem for our discussion because the average cell growth rate for equivalent-dose conditions was similar in different chambers (Fig. S2, ESI[†]). Although the cell growth rate change may increase the protein expression to a higher value, it does not affect the ranking of the proteins based on the *R* value. In conclusion, our system provides a good method for studying the protein response to an external pheromone.

Our designed microfluidic chip is a powerful tool for high-throughput microfluidic experiments; it allows investigation of the response of 48 proteins in two different extracellular environments at the same time on one chip. Our system guarantees that the yeast cells are in a similar environment which would enhance the comparability, convenience and repeatability of the experiment. Combined with a microscope system, our chip can easily detect protein expression and morphology changes with high time resolution and longer observation times than traditional methods. However, our method is not appropriate for very long observation times because daughter cells remain in the chambers. Although our chip is helpful for studying many biological processes, it is not suitable for researching fast protein regulation processes, protein modification processes and some space constraint sensitive process, such as yeast spore formation.

Besides microfluidic chips, it is easy to achieve batch processing for 96 chambers' pictures using our image processing program. In conclusion, this method would greatly shorten our image processing time and help to obtain large amounts of experimental data, which would contain much information about the related biological process, and the method is not limited to the mating process studied here.

Acknowledgements

We would like to thank Yugang Wang, Gen Yang, and Feng Liu for helpful discussion. This work is partially supported by the NSF of China (11174012 and 11434001).

References

- 1 R. E. Chen and J. Thorner, *Biochim. Biophys. Acta, Mol. Cell Res.*, 2007, **1773**, 1311–1340.
- 2 F. Naider and J. M. Becker, *Peptides*, 2004, **25**, 1441–1463.
- 3 L. Bardwell, *Peptides*, 2004, **25**, 1465–1476.
- 4 L. Merlini, O. Dudin and S. G. Martin, *Open Biol.*, 2013, **3**, 130008.
- 5 R. C. Yu, C. G. Pesce, A. Colman-Lerner, L. Lok, D. Pincus, E. Serra, M. Holl, K. Benjamin, A. Gordon and R. Brent, *Nature*, 2008, **456**, 755–761.
- 6 S. Paliwal, P. A. Iglesias, K. Campbell, Z. Hilioti, A. Groisman and A. Levchenko, *Nature*, 2007, **446**, 46–51.
- 7 S. Erdman and M. Snyder, *Genetics*, 2001, **159**, 919–928.
- 8 J. E. Segall, *Proc. Natl. Acad. Sci. U. S. A.*, 1993, **90**, 8332–8336.
- 9 C. J. Roberts, B. Nelson, M. J. Marton, R. Stoughton, M. R. Meyer, H. A. Bennett, Y. D. D. He, H. Y. Dai, W. L. Walker, T. R. Hughes, M. Tyers, C. Boone and S. H. Friend, *Science*, 2000, **287**, 873–880.
- 10 A. Gruhler, J. V. Olsen, S. Mohammed, P. Mortensen, N. J. Faergeman, M. Mann and O. N. Jensen, *Mol. Cell. Proteomics*, 2005, **4**, 310–327.
- 11 S. Erdman, L. Lin, M. Malczynski and M. Snyder, *J. Cell Biol.*, 1998, **140**, 461–483.
- 12 S. P. Gygi, Y. Rochon, B. R. Franza and R. Aebersold, *Mol. Cell. Biol.*, 1999, **19**, 1720–1730.
- 13 B. Futcher, G. I. Latter, P. Monardo, C. S. McLaughlin and J. I. Garrels, *Mol. Cell. Biol.*, 1999, **19**, 7357–7368.
- 14 M. C. Park, J. Y. Hur, H. S. Cho, S. H. Park and K. Y. Suh, *Lab Chip*, 2011, **11**, 79–86.
- 15 K. R. King, S. H. Wang, D. Irimia, A. Jayaraman, M. Toner and M. L. Yarmush, *Lab Chip*, 2007, **7**, 77–85.
- 16 R. J. Taylor, D. Falconnet, A. Niemisto, S. A. Ramsey, S. Prinz, I. Shmulevich, T. Galitski and C. L. Hansen, *Proc. Natl. Acad. Sci. U. S. A.*, 2009, **106**, 3758–3763.
- 17 W. K. Huh, J. V. Falvo, L. C. Gerke, A. S. Carroll, R. W. Howson, J. S. Weissman and E. K. O'Shea, *Nature*, 2003, **425**, 686–691.
- 18 J. Zeitlinger, I. Simon, C. T. Harbison, N. M. Hannett, T. L. Volkert, G. R. Fink and R. A. Young, *Cell*, 2003, **113**, 395–404.
- 19 J. R. Cheng and S. W. Foo, *IEEE Transactions on Image Processing*, 2006, **15**, 1563–1571.
- 20 N. Hao, S. Nayak, M. Behar, R. H. Shanks, M. J. Nagiec, B. Errede, J. Hasty, T. C. Elston and H. G. Dohlman, *Mol. Cell*, 2008, **30**, 649–656.
- 21 A.-C. Butty, P. M. Pryciak, L. S. Huang, I. Herskowitz and M. Peter, *Science*, 1998, **282**, 1511–1516.
- 22 V. Brizzio, A. E. Gammie, G. Nijbroek, S. Michaelis and M. D. Rose, *J. Cell Biol.*, 1996, **135**, 1727–1739.
- 23 S. Chou, S. Lane and H. P. Liu, *Mol. Cell. Biol.*, 2006, **26**, 4794–4805.
- 24 H. Ma, B. K. Han, M. Guaderrama, A. Aslanian, J. R. Yates, T. Hunter and C. Wittenberg, *Mol. Cell. Biol.*, 2014, **34**, 452–463.
- 25 P. G. Bertram, J. H. Choi, J. Carvalho, W. D. Ai, C. B. Zeng, T. F. Chan and X. F. S. Zheng, *J. Biol. Chem.*, 2000, **275**, 35727–35733.
- 26 J. E. Falk, A. C. H. Chan, E. Hoffmann and A. Hochwagen, *Dev. Cell*, 2010, **19**, 599–611.
- 27 U. S. Jung, A. K. Sobering, M. J. Romeo and D. E. Levin, *Mol. Microbiol.*, 2002, **46**, 781–789.
- 28 D. E. Levin, *Microbiol. Mol. Biol. Rev.*, 2005, **69**, 262–291.
- 29 D. Mack, K. Nishimura, B. K. Dennehey, T. Arbogast, J. Parkinson, A. Tohe, J. R. Pringle, A. Bender and Y. Matsui, *Mol. Cell. Biol.*, 1996, **16**, 4387–4395.
- 30 M. S. Singer, A. Kahana, A. J. Wolf, L. L. Meisinger, S. E. Peterson, C. Goggin, M. Mahowald and D. E. Gottschling, *Genetics*, 1998, **150**, 613–632.
- 31 C. Zhu, K. J. R. P. Byers, R. P. McCord, Z. W. Shi, M. F. Berger, D. E. Newburger, K. Saulrieta, Z. Smith, M. V. Shah, M. Radhakrishnan, A. A. Philippakis, Y. H. Hu, F. De Masi, M. Pacek, A. Rolfs, T. Murthy, J. LaBaer and M. L. Bulyk, *Genome Res.*, 2009, **19**, 556–566.
- 32 Y. Yu and J. P. Hirsch, *DNA Cell Biol.*, 1995, **14**, 411–418.
- 33 C. Cappellaro, C. Baldermann, R. Rachel and W. Tanner, *EMBO J.*, 1994, **13**, 4737–4744.
- 34 H. X. Xu, U. J. Kim, T. Schuster and M. Grunstein, *Mol. Cell. Biol.*, 1992, **12**, 5249–5259.
- 35 S. D. Johnston, S. Enomoto, L. Schneper, M. C. McClellan, F. Twu, N. D. Montgomery, S. A. Haney, J. R. Broach and J. Berman, *Mol. Cell. Biol.*, 2001, **21**, 1784–1794.
- 36 P. Friden and P. Schimmel, *Mol. Cell. Biol.*, 1987, **7**, 2708–2717.
- 37 K. C. Dobi and F. Winston, *Mol. Cell. Biol.*, 2007, **27**, 5575–5586.
- 38 V. Cloud, Y. L. Chan, J. Grubb, B. Budke and D. K. Bishop, *Science*, 2012, **337**, 1222–1225.